Wettability Investigations on the Cellulosic Surface of Alfa Fibers

N. Bohli,[1] A. Perwuelz,[2] R. Ben Cheikh,[1] M. Baklouti[1]

[1]Unité de Recherche en Synthèse et Analyse des Matériaux, Ecole Nationale d'Ingénieurs de Tunis, BP 37, Le Belvédère, 1002 Tunis, Tunisia
[2]Ecole Nationale Supérieure des Arts et Industries Textiles, Laboratoire de Génie et Matériaux Textiles, 9 Rue de l'Ermitage, BP 30329, 59056 Roubaix Cedex 01, France

ABSTRACT: A wettability study was performed on samples of alfa fibers with the Wilhelmy plate technique. The set of test liquids employed in the measurement of the contact angles was composed of water, heptane, diiodomethane, α-bromonaphthalene, and formamide. During their first immersion in high-surface-energy test liquids, the alfa fibers showed anisotropic behavior: they had an advancing contact angle of $67 \pm 6°$ in one orientation of immersion and an angle of $112 \pm 9.5°$ in the opposite one. Optical microscopy revealed the existence of fibrils on the alfa-fiber surface. They kept almost the same orientation and were responsible for the interesting hydrophobic/hydrophilic behavior of the fibers. Contact angle measurements and investigations of the hysteresis were also performed. The various results were examined according to the heterogeneities of the fibers. The surface energy of the alfa fibers was determined with three theoretical models: the geometric model, the Good–Van Oss–Chaudhury model, and the Chang model. A comparative study of these models was undertaken. The study of the wetting properties of alfa fibers will provide essential information for optimized composites and so will help us in choosing the right chemical treatment necessary to enhance adhesion in alfa-fiber-based composites. © 2008 Wiley Periodicals, Inc. J Appl Polym Sci 110: 3322–3327, 2008

Key words: biofibers; surface; adhesion; structure–property relations

INTRODUCTION

For economic and ecological reasons, interest in natural fibers has been growing for the last 2 decades. The interesting performances of natural-fiber-based composites have enhanced this interest. The investigations in this field have ranged from common natural fibers such as cotton,[1] sisal,[2] jute,[3] and wood[4] to more uncommon ones such as palm tree fibers.[5] In addition to giving rise to well-performing material composites, these fibers bring new challenges related to the improvement of the adhesion and the compatibility at the fiber–matrix interface. Natural fibers often show a large degree of nonuniformity in most characteristics: chemical composition, crystallinity, surface properties, diameter, density cross-sectional shape, length, strength, and stiffness.[6] Thus, to come up with an optimized composite with excellent overall physical properties, it is crucial to investigate the physicochemical properties of the fiber surface.

In this study, we have chosen esparto grass, which is more commonly known as alfa fiber. This natural fiber grows mainly in the arid regions of North Africa. Previous studies on the mechanical performance of alfa/polyester composites have shown interesting results comparable to those obtained with E-glass/polyester composites: a tensile modulus of 4 GPa, a tensile strength of 41 MPa, and a deformation of 1.4%.[7] However, a better knowledge of the wetting properties of these fibers is needed to overcome the imperfect bonding that can occur in composite materials.

Alfa fibers are lignocellulosic fibers composed of cellulose (45%), hemicellulose (24%), lignin (24%), ash (2%), and wax (5%).[8] The wettability of lignocellulosic fibers has been widely studied by the research community. Generally, the presence of waxes and lignin at the surface leads to poor wettability. A contact angle of 60° with water has been reported for lignin. Cellulose, being much more polar, displays a contact angle of approximately 33° with water.[9] Surface energies of natural fibers strongly depend on the extraction methods, chemical treatments, and intrinsic heterogeneities. Therefore, the reported surface energies are quite widely distributed. Values reported for wood fibers vary between 30 and 37 mJ/m^2.[10] More cellulosic materials display a higher surface energy. For example, it has been reported to be 49.8 mJ/m^2 for cotton fibers.[1] In such materials, the high value of the polar component is responsible for those values.
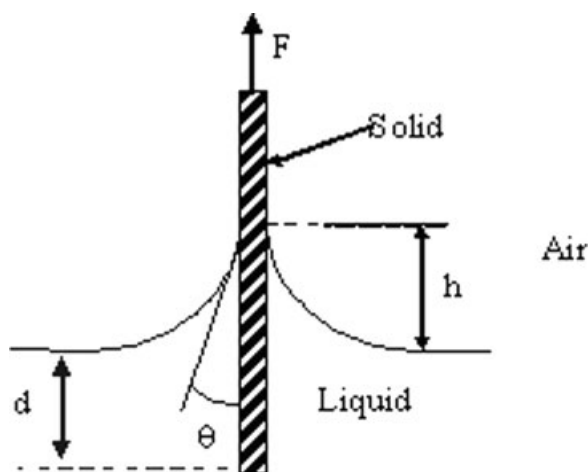
Figure 1 Measurements of the contact angle by the Wilhelmy technique.

Several techniques can be used for assessing a material's wetting properties. For example, we can use inverse gas chromatography,[11] electrokinetic analysis,[1] atomic force microscopy adhesion force measurements,[12] and dynamic contact angle measurements.[13] The last method was used in this study.

The aim of this study was to determine the surface energy of alfa fibers to quantify the interactions between these fibers and the matrices.

EXPERIMENTAL

Materials

For the extraction of the alfa fibers, we followed an optimized extraction process[14] to obtain long fibers with good mechanical properties. The α stems were cooked for 2 h in a 3N NaOH solution at 100°C under atmospheric pressure. The obtained cooked stems were then washed with water and bleached in a 40% NaClO solution for 1 h. Then, they were washed again with distilled water and dried in an oven at 50°C for 24 h. The resulting fibers were finally ripped. The obtained fibers had a density of 0.5 g/cm^3 and a κ index of 20.6.

Dynamic contact angle technique

For the determination of the dynamic contact angles, a Cahn DCA 322 tensiometer (Cahn Instruments Inc.) was used. The test liquid was put in a 25-mL beaker. The Wilhelmy gravitational technique[15,16] consisted of dipping single fibers into the test liquid at a low speed (50.3 μm/s) up to a depth of 4–5 mm and then withdrawing them from the liquid at the same speed. The dynamic wetting forces were recorded with an electronic microbalance (see Fig. 1). The contact angle, calculated from changes in the wetting force (F), was determined as follows:

$$F = P\gamma_L \cos\theta - V\rho g \tag{1}$$

where P is the fiber perimeter, γ_L is the surface tension of the liquid at the liquid/air interface, V is the volume of the fiber immersed in the liquid, ρ is the density difference between the liquid and vapor phases, g is the acceleration due to gravity, and θ is the contact angle between the liquid and fiber material. As we were dealing with small fibers, the term $-V\rho g$ could be neglected.[1] Therefore, the equation became

$$F = P\gamma_L \cos\theta \tag{2}$$

The alfa-fiber surface free energy (γ^T) was determined with the Young–Dupres equation [eq. (3)][17] together with one of three theoretical models: the geometric mean model [eq. (4)], the Good–Van Oss–Chaudhury (GVOC) model [eq. (6)], or the Chang model [eq. (8)]:[9,18–20]

$$W_a = (1 + \cos\theta)\gamma_L \tag{3}$$

$$W_a = 2(\gamma_L^d \gamma_S^d)^{1/2} + 2(\gamma_L^p \gamma_S^p)^{1/2} \tag{4}$$

$$\gamma^T = \gamma^d + \gamma^p \tag{5}$$

$$W_a = 2\sqrt{\gamma_S^{LW}\ \gamma_L^{LW}} + 2\sqrt{\gamma_S^+\ \gamma_L^-} + 2\sqrt{\gamma_L^+\ \gamma_S^-} \tag{6}$$

$$\gamma^T = \gamma^{LW} + \gamma^{ab}, \gamma^{ab} = 2(\gamma^+\gamma^-)^{1/2} \tag{7}$$

$$W_a = (P_L^d P_S^d) - (P_L^a)(P_S^b) - (P_L^b)(P_S^a) \tag{8}$$

where θ is the contact angle; γ_L is the liquid surface free energy; γ_S is the solid surface free energy; γ^d is the dispersive surface free energy; γ^p is the polar surface free energy; γ^{LW} is the Lifshitz–van der Waals surface free energy; γ^+ and γ^- are the Lewis acid and Lewis base surface free energy terms, respectively; P_L^d and P_S^d are the dispersive parameters of the liquid and solid; P_L^a and P_L^b are the principal acid–base values of the liquid; and P_S^a and P_S^b are the principal acid–base parameters of the solid.

The advantage of the Chang model over the GVOC model is that it allows negative acid–base interactions.

Through the measurement of the dynamic contact angle with nonpolar liquid probes and polar liquid probes with known parameters, the solid surface energy components γ^{LW}, γ^+, and γ^- could be determined. As probe liquids, we used water, α-bromonaphthalene, heptane, diiodomethane, and formamide (analytical-reagent quality). The data for the surface energy components of the probe liquids are given in Table I.

Each tested alfa fiber was submitted to testing for a determined number of test cycles in several probe liquids following this order: heptane (one cycle) →

<div align="center">

TABLE I
Surface Energy Components of the Test Liquids (mJ/m²)

</div>

	Water	CH$_2$I$_2$	Formamide	α-Bromonaphthalene	Heptane
$\gamma_{experimental}$	72.7	50.8	56.8	40.6	20.3
$\gamma_{theoretical}$	72.8	50.8	58	44.4	20.8
γ_{LW}/γ^d	21.8	50.8	39	43.5	20.8
γ_{AB}/γ^p	51	0	19	—	0
γ^+	25.5	0	2.28	—	0
γ^-	25.5	0	39.6	—	0
P^d	6.6	11.6	7.3	10.5	—
P^a	6.88	−4.11	6.92	−2.67	—
P^b	−7.4	−4.12	−4.64	−3.82	—

water (two cycles) → heptane (two cycles) → CH$_2$I$_2$ (three cycles) → heptane (one cycle) → α-bromo-naphthalene (three cycles) → heptane (one cycle) → formamide (three cycles). Therefore, after each immersion in a given test liquid, the alfa fiber was immersed in heptane to ensure that any residue of the previous test liquid was washed off.

RESULTS AND DISCUSSION

Macroscopic heterogeneities: the advancing contact angle on one fiber

The perimeter variation with the fiber length is shown in Figure 2. A precise value of the perimeter of the alfa fibers was calculated with the data recorded for heptane. In fact, as heptane has a very low surface energy, we assumed that it would completely wet the alfa fiber (cos $\theta_R = 1$). From Figure 2, it appears that the perimeter varies from 0.6 to 0.8 mL along the fiber axis. This is probably due to the existence of macroscopic heterogeneities resulting from the extraction process. The variation of the cosine of the advancing contact angle (cos θ) with the fiber length is also given in Figure 2 for water, diio-

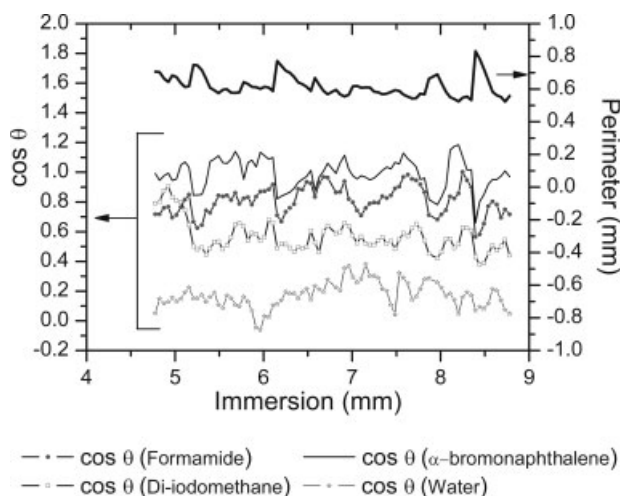domethane, α-bromonaphthalene, and formamide. With nonwetting liquids, the advancing contact angle along the fiber axis is deduced from the advancing wetting force of the liquid and from the real perimeter given previously [eq. (2)]. Each increase in the perimeter corresponds to a decrease in cos θ with dispersive liquids such as CH$_2$I$_2$, α-bromonaphthalene, and formamide.

At each point of the fiber, the surface energy and its components can be calculated from the liquid contact angles with, for example, the GVOC model. The evolution of the dispersive surface energy component of the alfa fiber and the perimeter along the whole length of one fiber are shown in Figure 3. The dispersive surface energy is about 40 mJ/m². For regions corresponding to an increase in the perimeter, there is a decrease in the dispersive surface energy of about 8 mJ/m².

In conclusion, this experimental study of a single fiber shows that the fiber surface has macroscopic heterogeneities. The fiber perimeter is not constant. An increase in the perimeter corresponds to a decrease in the surface energy and especially in the dispersive component. These bumps responsible for the increase in the perimeter at the alfa-fiber surface have a lower surface energy than other areas of the
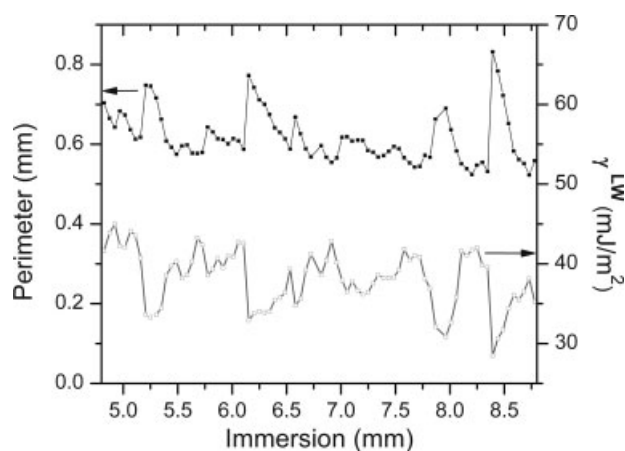
Figure 2 Evolution of cos θ between each test liquid and one alfa fiber with the perimeter.

Figure 3 Evolution of the dispersive surface energy component (GVOC model) along the length of one alfa fiber.
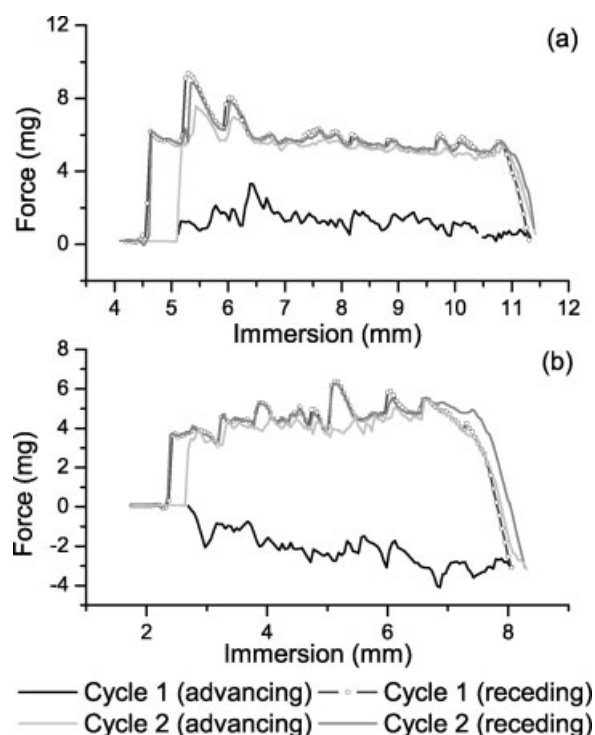
Figure 4 Tensiogram of one alfa fiber in distilled water: (a) hydrophilic orientation and (b) hydrophobic orientation.

fiber. Therefore, they may be waxes or lipid species that could not be removed during the extraction process.

Microscopic heterogeneities

All the studied fibers have heterogeneities, as described previously. However, the water wetting behavior reveals another type of heterogeneity on a microscopic scale.

Water advancing wetting analysis on one fiber

Two cycles of advancing and receding forces along one alfa fiber in distilled water are presented in Figure 4, which provides two different results depending on the orientation of the fiber. On both tensiograms, the first advancing force is much smaller than the receding one; this is known as wetting hysteresis. The low wetting force recorded for the first advancing cycle becomes higher for the other cycles of immersion and receding, probably because of the presence of adsorbed water at the fiber surface.

Let us consider the behavior of the alfa fiber during its first advancing contact angle phase in distilled water. Depending on the orientation of immersion of the fiber, either a hydrophilic response [Fig. 4(a)] or a hydrophobic response [Fig. 4(b)] could be found. The calculated advancing contact angle was estimated to be $67 \pm 6°$ in one orientation

of immersion (the K direction) and $112 \pm 9.5°$ in the opposite orientation (the K' direction).

Optical microscopy of alfa fibers

The optical microscopy of the surface of alfa fibers revealed the existence of oriented fibrils [Fig. 5(a,b)]. One very plausible explanation for the hydrophobic/hydrophilic behavior may be the presence of those heterogeneities intrinsically existing on the surface of the fibers. Depending on the orientation of the fibrils with respect to the wetting direction, the wetting will be different. If the fibrils are not in
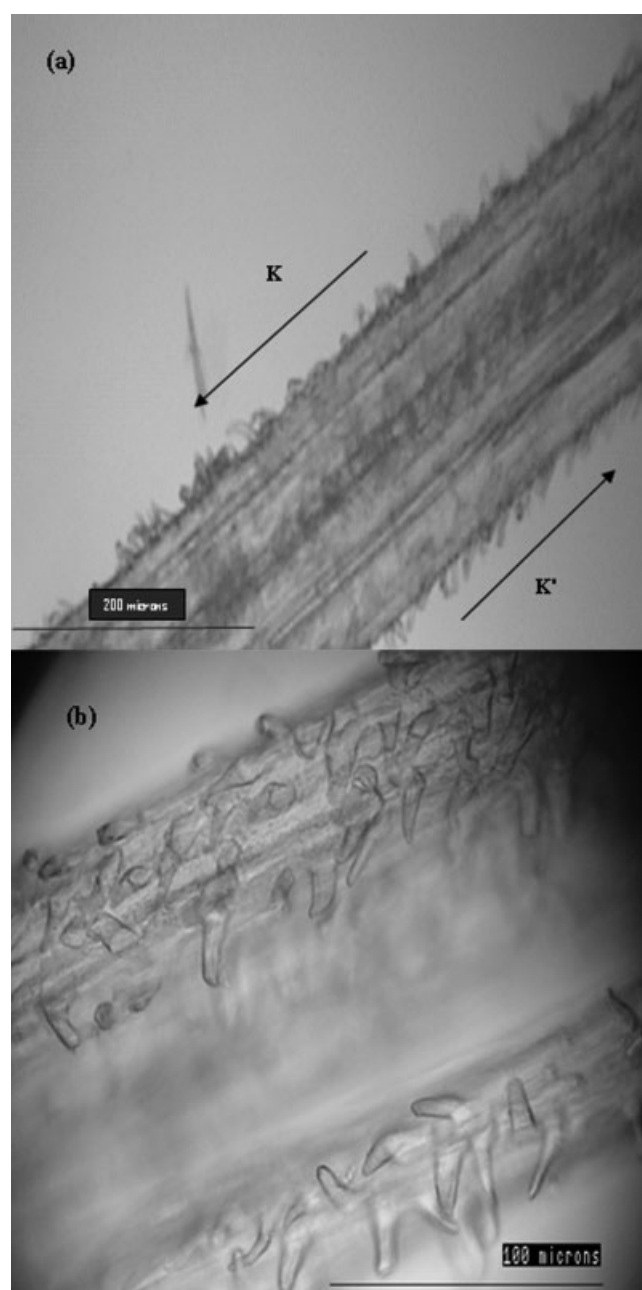

Figure 5 Optical microscopy of alfa fibers: (a) $10\times$ and (b) $40\times$.
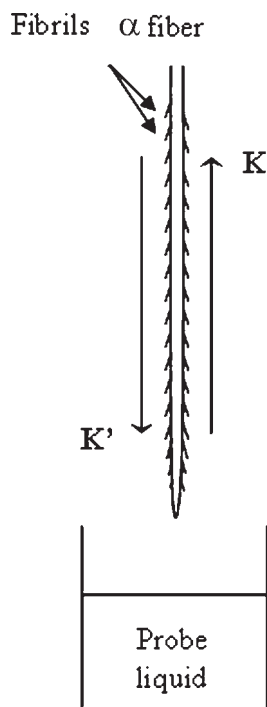
Fibrils α fiber

K

K'

Probe liquid

Figure 6 Definition of K and K' directions.

the same direction as the wetting one (the K' direction), liquids will have to wet the interstices between the fiber and the fibril. The low-wetting liquids will have difficulty in filling those narrow spaces. However, this will be much easier for low-surface-energy liquids, which have a contact angle close to zero. In fact, further experiments with different test liquids have shown that the hydrophilic/hydrophobic response is observed only with highly polar test liquids. If the fibrils are oriented in the same direction as the wetting direction (the K direction), this will not happen.

The water wetting behavior of alfa fibers is affected by the presence of oriented fibrils on the fiber surface. Depending on the orientation of the fibrils toward the wetting orientation, the fiber can be either hydrophobic (the K' direction) or hydrophilic (the K direction). This notation is defined more clearly in Figure 6.

Water advancing wetting analysis on different fibers

To get a better understanding of this hydrophilic/hydrophobic behavior of alfa fibers, an experiment was performed with four fibers. The advancing contact angle obtained during the first immersion in water of these fibers is presented in Table II.

We note that the contact angle of the alfa fiber varies with the perimeter. The alfa-fiber perimeter depends mainly on two conditions: the extraction process and the initial position of the fiber in the stem. Fibers cut from the bottom of the stem have a

lower perimeter than those cut from the top of the stem. The orientation of the fibers has a strong impact on the contact angle: in the K direction, the contact angle varies between 0.3 and 0.5. The difference is more significant in the K' direction: $\cos \theta = -0.6$ on lower perimeter fibers versus $\cos \theta = -0.1$ on higher perimeter fibers. At the top of the α stem, the hydrophilic/hydrophobic behavior is enhanced in comparison with the bottom, at which there is a smaller effect of the orientation.

Surface energy of alfa fibers

The mean surface energy and its components were evaluated from the advancing contact angle measurements of seven fibers in the K direction. For each fiber, about 100 contact angles were determined for each liquid. The obtained values included the macroscopic heterogeneities described previously. Table III lists the surface energy components of the alfa fibers calculated with the three different models. The geometric mean model gives different results depending on the polar liquids combination.[6,9] This table shows quite high standard deviations, particularly for the nondispersive components of surface energy. This is mainly due to the fiber heterogeneities, as pointed out previously, and heterogeneities between fibers. The latter are clearly displayed in Figure 7(a), in which the dispersive components of fibers vary from 26 to 40 mJ/m^2 for the GVOC model. The variations are mainly due to nondispersive components [5–15; see Fig. 7(b)].

When the results of the three models are compared, it is obvious that the Chang model does not agree with the others.

The geometric model and GVOC model give close results. According to the GVOC model, basicity dominates the alfa-fiber surface. Those results agree with the study by Gardner et al.[20] on wood fibers. This is probably a result of the NaOH treatment during fiber extraction. The surface energy of alfa fibers is about 42 mJ/m^2, which is comparable to the

TABLE II
Advancing Contact Angles of alfa fibers During the First Immersion in Distilled Water

Fiber	Direction of immersion	Perimeter (mm)	$\cos \theta_{water}$[a]
1	K'	0.5	-0.6 ± 0.2
	K	0.6	0.5 ± 0.1
2	K'	0.5	-0.6 ± 0.1
	K	0.5	0.3 ± 0.1
3	K'	0.9	-0.1 ± 0.2
	K	1.0	0.4 ± 0.1
4	K'	1.0	-0.009 ± 0.086
	K	1.1	0.4 ± 0.1

[a] A mean value of over 100 collected data.

TABLE III
Surface Energy Components of the alfa fiber (mJ/m²)

Model	Test liquid combination	γ_s^{LW}	γ_s^- base/P^b	γ_s^+ acid/P^a	γ_s^{ab}	γ_s^T
Geometric	CH₂I₂/α-bromonaphthalene/water	33.6 ± 5	—	—	12.2 ± 3.6	45.8 ± 7
	CH₂I₂/α-bromonaphthalene/formamide	33.6 ± 5	—	—	9.8 ± 4.5	43.4 ± 6.5
	CH₂I₂/α-bromonaphthalene/water/formamide (linear regression)	32.5 ± 4.8	—	—	11.8 ± 3.4	44.3 ± 6.6
GVOC	CH₂I₂/α-bromonaphthalene/water/formamide	33.3 ± 5	13.6 ± 5.7	1.8 ± 1.7	8.9 ± 2.6	42.2 ± 6.1
Chang	CH₂I₂/α-bromonaphthalene/water/formamide	27.1 ± 6.5	−4.4 ± 0.7	3.3 ± 1.8	13.8 ± 7.3	40.9 ± 6

values found in the literature for natural fibers.[12] The Lifshitz–van der Waals surface energy component mean value is 33 mJ/m² for the GVOC model. Estimates of the nondispersive component range from 9 to 14 mJ/m², and this is attributed to the —OH group of the cellulose. The total surface energies of alfa fibers determined by the geometric and GVOC models are comparable within ~2 mJ/m².

CONCLUSIONS

The heterogeneities of alfa fiber are displayed on both microscopic and macroscopic levels. The former is due to the existence of oriented fibrils on the fiber surface revealed by dynamic contact angle analyses and optical investigations, which provide the fibers with an interesting hydrophobic/hydrophilic wett-

ability response. The latter is more likely due to the irregularities of the fibers. Therefore, more attention must be taken during the extraction process to obtain better homogenized alfa fibers.

The surface energy components of these natural fibers were calculated with three different mathematical models. In comparison with the Chang model and the mean geometric model, the GVOC model seems to give a precise estimation of the surface energy components. The alfa fibers showed basic surfaces with a total surface energy estimated to ~42 mJ/m². This value is in agreement with values found for natural fibers in the literature.

Figure 7 Surface energy components of seven alfa fibers: (a) dispersive surface energies and (b) polar surface energies.

References

1. Buschle-Diller, G.; Inglesby, M. K.; Wu, Y. Colloids Surf A 2005, 260, 63.
2. Li, Y.; Mai, Y. W.; Ye, L. Compos Sci Technol 2000, 60, 2037.
3. Gassan, J. Compos A 2002, 33, 369.
4. Wålinder, M. Doctoral Thesis, Stockholm KTH-Royal Institute of Technology, 2000.
5. Kaddami, H.; Dufresne, A.; Khelifi, B.; Bendahou, A.; Taourirte, M.; Raihane, M.; Issartel, N.; Sautereau, H.; Gérard, J. F.; Sami, N. Compos A 2006, 37, 1413.
6. Bledzki, A.; Gassan, J. Prog Polym Sci 1999, 24, 221.
7. Ben Brahim, S.; Ben Cheikh, R. Compos Sci Technol 2007, 67, 140.
8. (a) Bledzki, A. K.; Gassan, J. Natural Fiber Reinforced Plastics; University of Kassel: Kassel, Germany, 1996; (b) Ben Brahim, S.; Ben Cheikh, R. Compos Sci Technol 2007, 67, 140.
9. Gassan, J.; Gutowski, V. S.; Bledzki, A. Macromol Mater Eng 2000, 283, 132.
10. Barsberg, S.; Thygesen, L. G. J Colloid Interface Sci 2001, 234, 59.
11. Tshablala, M. A. J Appl Polym Sci 1997, 65, 1013.
12. Pietak, A.; Korte, S.; Tan, E.; Downard, A.; Staiger, M. P. Appl Surf Sci 2007, 253, 3627.
13. Van de Velde, K.; Kiekens, P. Angew Makromol Chem 1999, 272, 87.
14. Ben Cheikh, R.; Ben Brahim, S.; Baklouti, M. International Conference on Composite Materials 13, Beijing, China, June 2001; No. 1620.
15. Son, J.; Gardner, D. J Wood Fibre Sci 2004, 36, 98.
16. Bendure, R. L. J Colloid Interface Sci 1973, 42, 137.
17. Dupré, A. Théorie Mécanique de la Chaleur; Gauthier-Villars: Paris, 1869; p 367.
18. Owens, D. K.; Wendt, R. C. J Appl Polym Sci 1969, 13, 1741.
19. Good, R. J.; Chaudhury, M. K.; Van Oss, C. J. In Fundamentals of Adhesion; Lee, L.-H., Ed.; Plenum: New York, 1991; Chapter 4.
20. Gardner, D. J.; Shi, S. Q.; Tze, W. T. Presented at the 2nd International Symposium on Acid–Base Interactions: Releva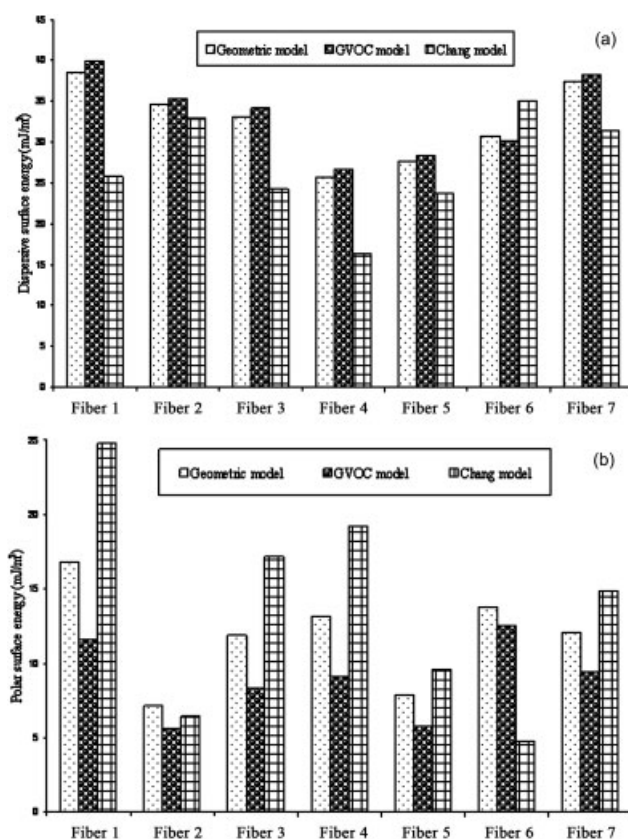nce to Adhesion, Newark, NJ, 1998.